inorganics

MDPI

Communication

Monodentate Ligands in X-Cu(I)-Y Complexes—Structural Aspects

Milan Melník [1,*], Veronika Mikušová [2] and Peter Mikuš [1,3,*]

[1] Department of Pharmaceutical Analysis and Nuclear Pharmacy, Faculty of Pharmacy, Comenius University Bratislava, Odbojárov 10, SK-832 32 Bratislava, Slovakia
[2] Department of Galenic Pharmacy, Faculty of Pharmacy, Comenius University Bratislava, Odbojárov 10, SK-832 32 Bratislava, Slovakia; mikusova@fpharm.uniba.sk
[3] Toxicological and Antidoping Centre, Faculty of Pharmacy, Comenius University Bratislava, Odbojárov 10, SK-832 32 Bratislava, Slovakia
* Correspondence: qmelnik@stuba.sk (M.M.); mikus@fpharm.uniba.sk (P.M.)

Abstract: This structural study examines over 102 coordinate Cu(I) complexes with compositions such as C-Cu-Y (Y=HL, OL, NL, SL, SiL, BL, PL, Cl, Br, I, AlL, or SnL), N-Cu-Y (Y=OL, Cl), S-Cu-Y (Y=Cl, Br, I), P-Cu-Y (Y=Cl, I), and Se-Cu-Y (Y=Br, I). These complexes crystallize into three different crystal classes: monoclinic (seventy-two instances), triclinic (twenty-eight instances), and orthorhombic (eight instances). The Cu-L bond length increases with the covalent radius of the ligating atom. There are two possible geometries for coordination number two: linear and bent. A total of 21 varieties of inner coordination spheres exist, categorized into two hetero-types (C-Cu-Y, i.e., organometallic compounds and X-Cu-Y, i.e., coordination compounds). The structural parameters of hetero Cu(I) complexes were compared with trans-X-Cu (I)-X (homo) complexes and analyzed. The maximum deviations from linearity (180.0°) are, on average, 10.3° for Br-Cu(I)-Br, 16.6° for C-Cu(I)-Sn, and 35.5° for P-Cu(I)-I. These results indicate that ligand properties influence deviation from linearity, increasing in the order of hard < borderline < soft.

Keywords: structural analysis; X-Cu(I)-Y complexes; monodentate ligands; trans-effect

Citation: Melník, M.; Mikušová, V.; Mikuš, P. Monodentate Ligands in X-Cu(I)-Y Complexes—Structural Aspects. *Inorganics* **2024**, *12*, 279. https://doi.org/10.3390/inorganics12110279

Academic Editors: Francis Verpoort, Axel Klein and Shuang Xiao

Received: 3 October 2024
Revised: 24 October 2024
Accepted: 26 October 2024
Published: 30 October 2024

1. Introduction

The chemistry of copper compounds has been widely studied, with a significant focus on the relationship between their structure and reactivity, which plays a crucial role in applications ranging from industrial catalysis to biomedical fields. Most X-ray studies of transition metal compounds involve copper. While copper typically exists in the +2 oxidation state, other states, including +1, +3, and +4, are also known, with copper(I) being the most common. Although copper(I) is prone to air oxidation and unstable in aqueous solutions, many stable compounds have been synthesized using soft pi-acid ligands, and others remain stable due to their very low solubility.

It is well-established that Cu(I) and Cu(II) complexes exhibit distinct intrinsic stereochemical preferences [1]. Copper(II), with its d9 configuration, tends to adopt stereochemistries that benefit from ligand field stabilization due to energetically favorable d-orbital splitting. In contrast, copper(I), being d10, has its stereochemistry primarily influenced by steric and charge effects alone. These differences in stereochemical preferences have significant implications for copper's role in biological redox chemistry. Blue copper proteins exemplify this by adopting a donor ligand set and stereochemistry that strike a balance between the inherent preferences of both copper(I) and copper(II) [2]. Studying the reaction chemistry of coordinatively unsaturated copper(I) complexes is key to understanding the reaction mechanism by which dioxygen-activating copper proteins function. Cuprous forms of these enzymes often exhibit two- or three-coordination [3]. Structural comparisons between copper(I) and copper(II) redox pairs have been reported with ligands like thioether [4–6], imidazole [7], and mixed pyridine thioether donors [8].

Structural studies of copper(I) compounds have been carried out and have been sporadically summarized in annual reports [9–12]. The structural chemistry of single halo (amine) copper(I) compounds has been reviewed [13]. A comprehensive overview of copper(I) structures (almost one thousand) was published in 1995 [14]. Recently, structures of mutually trans-X-Cu(I)-X (X=OL, NL, CL, PL, SL, Se L, Cl, or Br) were studied [15]. This manuscript aims to analyze the structural parameters of over one hundred X-Cu(I)-Y complexes, enabling us to compare them with the previously analyzed group of X-Cu(I)-X complexes. The structures are divided into two groups according to their coordination atoms: C-Cu(I)-Y and X-Cu(I)-Y, respectively.

2. Structural Aspects of C-Cu(I)-Y (Y=HL, OL, NL, SL, Si L, BL, PL, Cl, Br, I, CAl, or CSn)

2.1. Structures of C-Cu(I)-Y (Y=HL, OL)

In the monoclinic 0.55 ($C_{22}H_{36}N^+$) 0.55 ($C_{18}HBF_{15}^-$) 0.45 [Cu($C_{22}H_{36}N$)($C_{18}HBF_{15}$)] (at 100 K) [16], two unidentate ligands, in the former via C- and in the latter via H-donor atoms, form the C-Cu(I)-H type with Cu-L bond distances of 1.879 Å (L=C) and 1.769 Å (L=H). The C-Cu(I)-H bond angle is 177.0°. This is the only example of such a type.

There are 19 examples in which two unidentate ligands, via C- and O-donor atoms, form the C-Cu(I)-O type. Such Cu(I) complexes are the monoclinics [Cu($C_{22}H_{35}N$)(CHO_2)] (at 100 K) [16], [Cu($C_{18}H_{20}N_2$)(t-BuO)] (at 210 K) [17], [Cu($C_{28}H_{40}N_2$(t-BuO)] (at 150 K) [17], [Cu($C_{27}H_{37}N_2$)($C_{27}H_{36}N_2O_2$)] (at 150 K) [18], [Cu($C_{27}H_{36}N_2$)($C_2H_3O_2$]0.5(C_6H_6) (at 193 K) [19], [Cu($C_{21}H_{24}N_2$)($C_2H_3O_2$)] (at 295 K) [20] [Cu($C_{27}H_{38}N_2$)($C_2H_3O_2$)]C_6H_6 (at 295 K) [20], [Cu($C_{27}H_{38}N_2$)($C_2H_3O_2$)]C_7H_8 (at 200 K) [21], [Cu($C_{21}H_{26}N_2$)(CF_3CO_2)] (at 173 K) [22], [Cu($C_{27}H_{36}N_2$)(PhCOO)] (at 100 K) [23], [Cu($C_{27}H_{37}N_2$)($C_8H_7O_3$)](C_4H_8O) (at 173 K) [24], [Cu($C_{24}H_{28}N_2O_2$)(Ph_3SiO)] (at 150 K) [25], and [Cu($C_{27}H_{38}N_2$)($C_5H_3SO_2$)] (at 100 K) [26].

The triclinics are [Cu($C_{23}H_{30}N_2$)(C_4H_9O)] (at 210 K) [17], [Cu($C_{21}H_{26}N_2$)(C_4H_9O)]0.5(C_6H_6) (at 150 K) [17], and [Cu($C_{24}H_{35}N_2$)($C_{14}H_{13}O_2$)]0.5(C_4H_8O) (at 163 K) [27].

The structure of [Cu($C_{24}H_{28}N_2O_2$)(Ph_3SiO)] [25] is shown in Figure 1 as an example. The total mean Cu-L bond distances in Cu(I) complexes with the C-Cu(I)-O type are 1.869 Å (range 1.844–1.886 Å) (L=C) and 1.837 Å (range 1.769–1.914 Å) (L=O). The C-Cu(I)-O bond angles range from 168.2° to 179.1° (mean 175.1°).

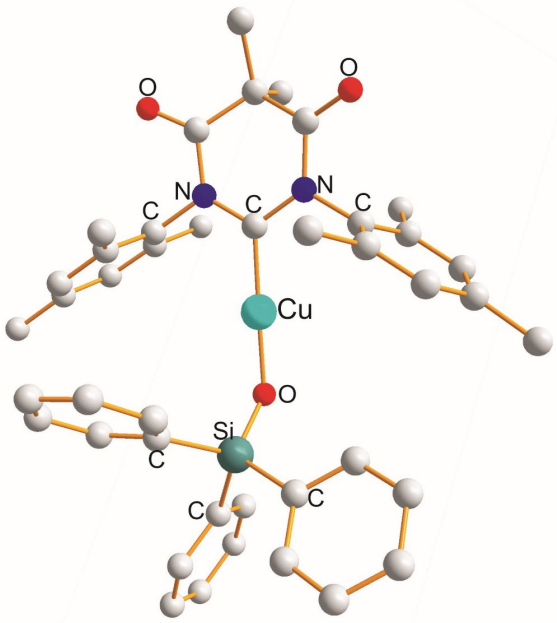

Figure 1. Structure of [Cu($C_{24}H_{28}N_2O_2$) (Ph_3SiO)] [25].

The [Cu($C_{11}H_{20}N_2$)(C_4H_9O)] (at 100 K) [27] complex crystallizes in two crystal classes, monoclinic and orthorhombic. Each Cu(I) atom has two coordinates (C-Cu(I)-O). These complexes also differ from the structural data. The Cu-L bond distances, monoclinic vs.

orthorhombic, are 1.876 Å (L=C) and 1.803 Å (L=O) vs. 1.882 Å and 1.815 Å. The values of the C-Cu(I)-O bond angles are 173.7° and 175.0°, respectively.

2.2. Structures of C-Cu(I)-Y (Y=NL, SL, SiL)

There are 21 Cu(I) complexes in which monodentate ligands, one via C atom and another one via N atom, create two-coordinate Cu(I) atoms of the C-Cu(I)-N type. Such complexes are the monoclinics $[Cu(C_{27}H_{36}N_2)(py)]BF_4$ (at 296 K) [28], $[Cu(C_{27}H_{36}N_2)(2\text{-}CH_3py)]BF_4CHCl_3$ (at 140 K) [28], $[Cu(C_{27}H_{36}N_2)(2\text{-}Phpy)]BF_4$ (at 140 K) [28], $[Cu(C_{27}H_{38}N_2)(t\text{-}Bu_3\ P{=}N)]C_6H_{14}$ (at 154 K) [29], $[Cu(C_{27}H_{36}N_2)(t\text{-}Bu_3\ P{=}N)]C_5H_{12}$ (at 200 K) [29], $[Cu(C_{23}H_{35}N)(C_{12}H_8N)]$ (at 100 K) [30], $[Cu(C_{28}H_{39}N_2)(C_{16}H_{17}PON)]$ (at 150 K) [31], $[Cu(C_{31}H_{38}N_2)(C_{12}H_8N)]$ (at 100 K) [32], $[Cu(C_{27}H_{36}N_2)(N_3)]$ (at 173 K) [33], $[Cu(C_{27}H_{36}N_2)(C_{12}H_8N)]$ (at 180 K) [34], $[Cu(C_{27}H_{34}N_2)(C_{12}D_8N)]$ (at 180 K) [34], and $[Cu(C_{19}H_{20}N_2)(NCO)]$ (at 293 K) [35], the orthorhombics $[Cu(C_{27}H_{34}N_2)(p\text{-}tosylN_4)]0.25(CH_2Cl_2)$ (at 173 K) [33], $[Cu(C_{21}H_{24}N_2)(C_{12}H_8N)]$ (at 180 K) [34], $[Cu(C_{27}H_{36}N_2)(NCO)]$ (at 123 K) [35], $[Cu(C_{27}H_{38}N_2)(NCO)]$ (at 123 K) [35], $[Cu(C_{27}H_{38}N_2)(NCS)]$ (at 123 K) [35], and $[Cu(C_{21}H_{24}N_2)(C_{11}H_{10}F_4NO_2)]$ (at 153 K) [36], and the triclinics $[Cu(C_{27}H_9N_2)(C_8H_7N_4O)]C_6H_6$ (at 173 K) [33], $[Cu(C_{27}H_{36}N_2)(C_8H_5N_2O)]$ (at 173 K) [33], and $[Cu(C_{11}H_{21}N_2)(C_{37}H_{63}AlN_4Si_2)]0.5(C_6H_{14})$ (at 150 K) [37]. The structure of $[Cu(C_{19}H_{20}N_2)(NCO)]$ [35] is shown in Figure 2 as an example. The total mean values of the Cu-L bond distances are 1.875 Å (range 1.862–1.928 Å) (L=C) and 1.864 Å (range 1.810–1.913 Å) (L=N) and the mean C-Cu(I)-N bond angle is 175.7° (range 166.8°–179.8°). The structure of $[Cu(C_{23}H_{35}N)(C_{12}H_8N)]$ [30] is shown in Figure 3 as another illustrative example.

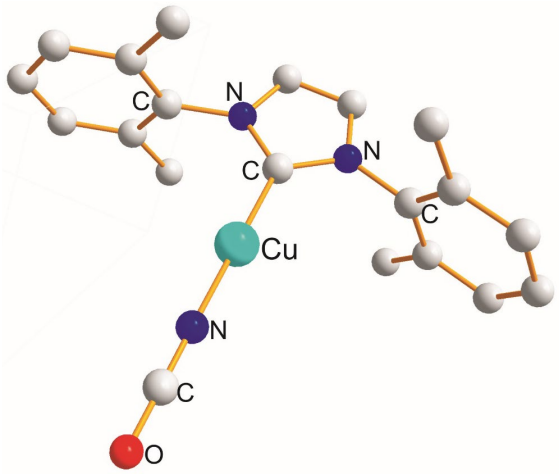

Figure 2. Structure of $[Cu(C_{19}H_{20}N_2)(NCO)]$ [35].

There are two Cu(I) complexes, the monoclinic $[Cu(C_{69}H_{56}N_2)(SH)]CH_2Cl_2$ (at 100 K) [38] and the orthorhombic $[Cu(C_{27}H_{36}N_2)(SH)]$ (at 100 K) [38], in which there is an unidentate ligand via a C-donor atom with an unidentate SH form of the C-Cu(I)-S type, with mean Cu-L bond distances of 1.867 Å (L=C) and 2.104 Å (L=S). The mean C-Cu(I)-S bond angle is 177.8°.

In the monoclinics $[Cu(C_{27}H_{36}N_2)((MeO)_3Si)]$ (at 100 K) [39], $[Cu(C_{21}H_{24}N_2)(C_8H_{11}Si)]$ (at 100 K) [40], $[Cu(C_{11}H_{20}N_2)(C_8H_{11}Si)]0.5C_7H_8$ (at 100 K) [40], $[Cu(C_{27}H_{36}N_2)(C_{21}HN_3Si_3)]$ SbF_6 CH_2Cl_2 (at 100 K) [41], the orthorhombics $[Cu(C_{21}H_{24}N_2)(Ph_3Si)]$ (at 100 K) [40] and $[Cu(C_{11}H_{20}N_2)(C_8H_{11}Si)]$ (at 100 K) [40], and the triclinic $[Cu(C_{27}H_{36}N_2)(Ph_3Si)]$ (at 100 K) [40], unidentate ligands via C- and Si-donor atoms form the C-Cu(I)-Si type. The structure of $[Cu(C_{27}H_{36}N_2)((MeO)_3Si)]$ [39] is shown in Figure 4 as an example. The total mean values of the Cu-L bond distances are 1.935 Å (range 1.925–1.941 Å) (L=C) and 2.273 (range 2.267–2.241 Å) (L=Si). The mean value of the C-Cu(I)-Si bond angles is 173.7 (range 168.2–178.5°).

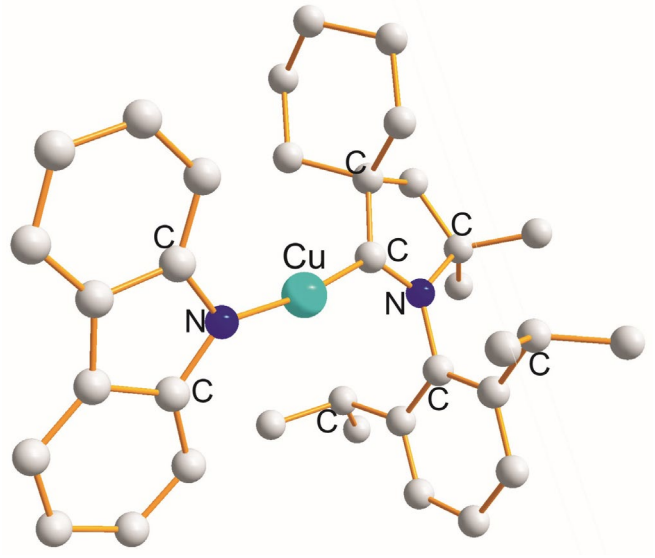

Figure 3. Structure of [Cu($C_{23}H_{35}N$)($C_{12}H_8N$)] [30].

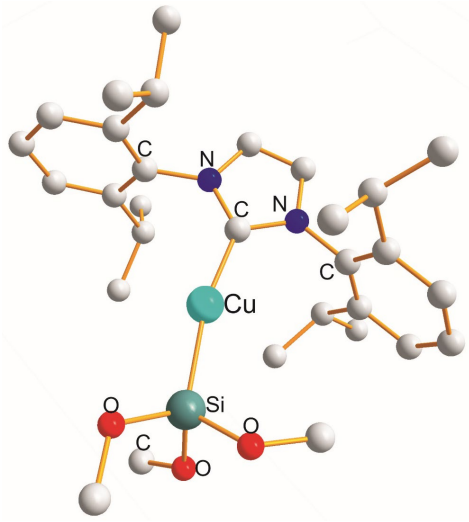

Figure 4. Structure of [Cu($C_{27}H_{36}N_2$)(($MeO)_3Si$)] [39].

2.3. Structures of C-Cu(I)-Y (Y=BL, PL)

There are four complexes: the monoclinics [Cu($C_{11}H_{20}N_2$)($C_8H_{10}N_2B$)] (at 100 K) [42] and [Cu($C_{27}H_{36}N_2$)($C_5H_{10}O_2B$)](C_4H_8O) (at 100 K) [43], the orthorhombic [Cu($C_{69}H_{56}N_2$)($C_5H_{10}O_2B$)] (at 100 K) [43], and the triclinic [Cu($C_{27}H_{36}N_2$)($C_5H_{10}O_2B$)]C_7H_8 (at 100 K) [43], in which unidentate ligands via C- and B-donor atoms form a C-Cu(I)-B type. The total mean values of the Cu-L bond distances are 1.939 (range 1.931–1.953 Å) (L=C) and 2.005 (range 1.993–2.020 Å) (L=B). The mean value of the C-Cu(I)-B bond angles is 173.5° (range 171.4–175.5°).

The two unidentate ligands, one via C- and another one via P-donor atom, create two-coordinate Cu(I) atoms (C-Cu(I)-Cl). There are seven complexes with such a type: the monoclinics [Cu($C_{27}H_{36}N_2$)($C_6H_{18}Si_2P$)]C_7H_8 (at 100 K) [44], [Cu($C_{27}H_{40}N$)($C_{22}H_{39}N_4OP$)] (at 100 K) [45], [Cu($C_{27}H_{36}N_2$)($C_8H_{23}N_2BP$)]Et_2O (at 130 K) [46], [Cu($C_{60}H_{84}AlN_4O$)(t-Bu_3P)]C_6H_6 (at 150 K) [47], triclinic [Cu($C_{28}H_{40}N_2$)(Ph_2P)] (at 150 K) [31], and [Cu($C_{27}H_{36}N_2$)(Ph_2P)] (at 150 K) [31], and the orthorhombic [Cu($C_{24}H_{26}N_2O_2$)($C_{21}H_{24}P$)] (at 150 K) [47]. The structure of [Cu($C_{24}H_{26}N_2O_2$)($C_{21}H_{24}P$)] [48] is shown in Figure 5 as an example.

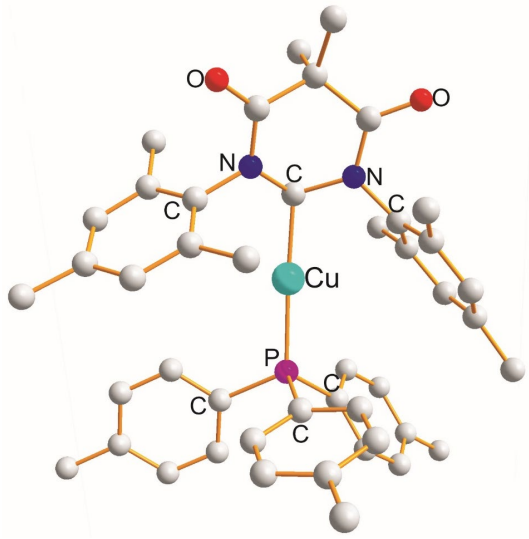

Figure 5. Structure of [Cu($C_{24}H_{26}N_2O_2$)($C_{21}H_{24}P$)] [48].

2.4. Structures of C-Cu(I)-Y (Y=Cl, Br, I, AlL, or SnL)

There are 16 Cu(I) complexes in which inner coordination spheres are built up by unidentate ligands via a C-donor atom with chloride (C-Cu(I)-Cl). These complexes crystalize in three crystal classes: monoclinic, orthorhombic, and triclinic. The monoclinics are [Cu($C_9H_{16}N_2$)(Cl)] (at 100 K) [49], [Cu($C_{30}H_{42}N_6$)(Cl)] (at 123 K) [50], [Cu($C_{22}H_{33}N$)(Cl)] (at 100 K) [51], [Cu($C_{45}H_{40}N_2$)(Cl)] (at 123 K) [52], [Cu($C_{45}H_{42}N_2$)(Cl)] (at 193 K) [53], [Cu($C_{19}H_{20}N_2$)(Cl)] (at 293 K) [54], [Cu($C_{20}H_{24}N_2S$)(Cl)]0.5CH_2Cl_2 (at 100 K) [55], [Cu($C_{20}H_{31}N$)(Cl)] (at 140 K) [56], [Cu($C_{21}H_{32}N_4$)(Cl)] (at 173 K) [57], [Cu($C_{30}H_{56}B_{11}N_3$)(Cl)] (at 296 K) [58], [Cu($C_{27}H_{43}N$)(Cl)] (at 100 K) [59], [Cu($C_{27}H_{43}N$)(Cl)] (at 100 K) [60], and [Cu($C_{27}H_{39}N$)(Cl)] (at 140 K) [60]; the orthorhombics are [Cu($C_{41}H_{38}N_2O_2$)(Cl)] (at 296 K) [61] and [Cu($C_{27}H_{30}N_2$)(Cl)] (at 150 K) [62]; and the triclinics are [Cu($C_{55}H_{44}N_2$)(Cl)] CH_2Cl_2(at 100 K) [63], [Cu($C_{21}H_{26}N_2O_2$) (Cl)] 0.25 (C_4H_8O) (at 150 K) [64], and [Cu($C_{32}H_{31}N$)(Cl)] (at 100 K) [65].

The structure of [Cu($C_{20}H_{24}N_2S$)(Cl)] [55] is shown in Figure 6 as an example. The total mean values of the Cu-L bond distances are 1.883 (range 1.869–1.892 Å) (L=C) and 2.100 (range 2.088–2.177 Å) (L=Cl). The total mean value of the C-Cu(I)-P bond angle is 175.9 (range 173.3–179.4°). The structure of [Cu($C_{27}H_{39}N$)(Cl)] (at 140 K) [60] is shown in Figure 7 as another illustrative example.

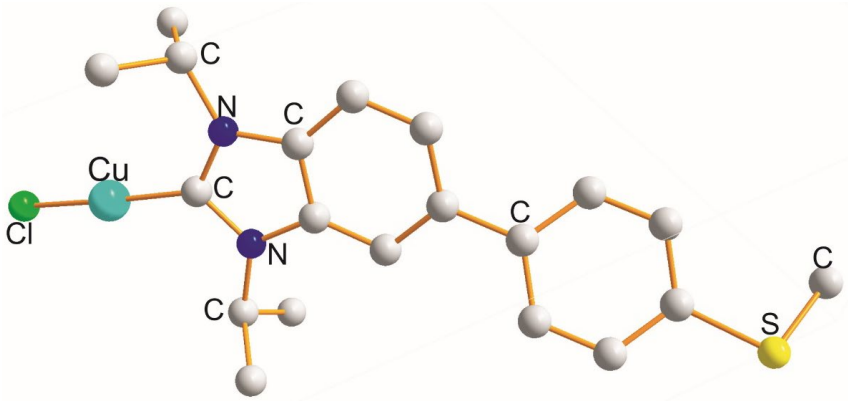

Figure 6. Structure of [Cu($C_{20}H_{24}N_2S$)(Cl)] [55].

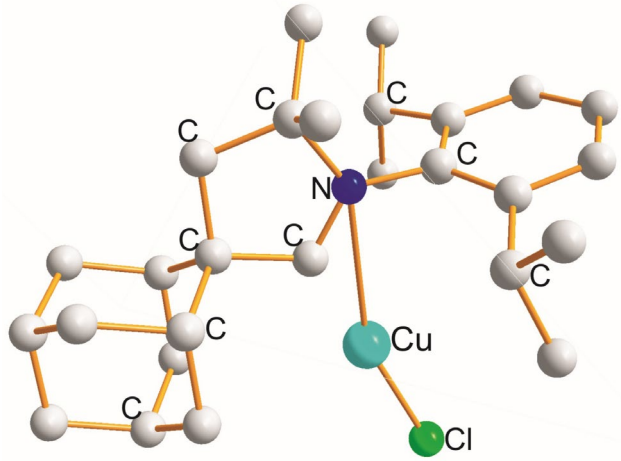

Figure 7. Structure of [Cu($C_{27}H_{39}N$)(Cl)] [60].

There are four monoclinic Cu(I) complexes, namely [Cu($C_{21}H_{16}N_2$)(Br)] (at 190 K) [66], [Cu($C_{40}H_4N_2ClP$)(Br)](CF_3SO_3)$_2$(CH_3CN) (at 173 K) [67], [Cu($C_{22}H_{21}F_5N_2$)(Br)] (at 100 K) [68], and [Cu($C_{31}H_{32}N_2$)(Br)] (at 295 K) [69], and one triclinic, namely [Cu($C_{32}H_{31}N$)(Br)] (at 100 K) [70], in which unidentate ligands via a C-donor atom with bromide build by two-coordinate inner spheres of C-Cu(I)-Br. The total mean values of the Cu-L bond distances are 1.892 (range 1.880–1.898 Å) (L=C) and 2.262 (range 2.216–2.268 Å) (L=Br). The total mean C-Cu(I)-Br bond angle is 174.8 (range 170.9–177.8°).

In the triclinics [Cu($C_{27}H_{39}N$)(I)]0.5CH_2Cl_2 (at 140 K) [60], [Cu($C_{27}H_{48}N_2O_3Si$)(I)] (at 100 K) [71], the monoclinic [Cu($C_8H_4N_2$)(I)] (at 298 K) [72], and the orthorhombic [Cu($C_{35}H_{36}N_2$)(I)] (at 133 K) [73], each unidentate ligand coordinated via a C-donor atom with iodine builds up an almost linear C-Cu(I)-I angle with a mean value of 178.9 (range 177.2–180°).

The total mean Cu-L bond distances are 1.915 (range 1.902–1.924 Å) (L=C) and 2.422 (range 2.416–2.42Å) (L=I).

There are two Cu(I) complexes, the monoclinic [Cu($C_{11}H_{21}N_2$)($C_{30}H_{50}N_2Si_2Al$)](C_7H_{14}) (at 150 K) [37] and the orthorhombic [Cu($C_{20}H_{31}N$)($C_{30}H_{50}N_2Si_2Al$)] (at 150 K) [37], in which two unidentate ligands, one via C- and another one via Al-donor atoms, build up almost linear C-Cu(I)-Al with bond angles of 175.9 (±25)°. The Cu-L bond distances are 1.958 (±5) Å (L=C) and 2.374 (±29) Å (L=Al).

The monoclinic [Cu($C_{27}H_{36}N_2$)(CH_3)$_3$ Sn)] (at 100 K) [40] is the only example of the C-Cu(I)-Sn type. The Cu-L bond distances are 1.925 Å (L=C) and 2.474 Å (L=Sn) and the C-Cu(I)-Sn bond angle is 163.4°.

3. Structural Aspects of X-Cu(I)-Y (X, Y = Variable Combination of Donor Atoms)

In the monoclinic [Cu($C_{30}H_{42}N_4$)(CH_3COO)] (at 213 K) [74] and triclinic [Cu($C_{40}H_{58}N_4$)(CH_3COO)] (at 213 K) [74], unidentate ligands create bent geometry via N- and O-donor atoms with a mean value of the N-Cu(I)-O angles of 162.8 (±5)°. The mean values of the Cu-L bond distances are 1.852 (±2) Å (L=N) and 1.842 (±2) Å (L=O).

The monoclinic [Cu($C_{13}H_{19}N_3O_2$)(Cl)] (at 130 K) [75] is the only example of the N-Cu(I)-Cl type. The N-Cu(I)-Cl bond angle is 170.6°and the Cu-L values are 1.885 Å (L=N) and 2.095 Å (L=Cl).

In two monoclinic Cu(I) complexes, [Cu($C_{21}H_{24}N_2S$)(Cl)] (at 298 K) [76] and [Cu($C_{27}H_{36}N_2S$)(Cl)] (at 100 K) [66], the united ligands via S-donor atom with chloride form a bent geometry about each Cu(I) atom (S-Cu(I)-Cl) with a value of 165.0 (±9)°. The mean values of the Cu-L bond distances are 2.139 (±9) Å (L=S) and 2.108 (±10) Å (L=Cl).

In three monoclinic Cu(I) complexes, [Cu($C_{21}H_{24}N_2S$)(Br)] (at 298 K) [76], [Cu($C_{27}H_{36}N_2S$)(Cl)] (at 100 K) [77], and [Cu($C_{69}H_{56}N_2S$)(Br)]C_7H_8 (at 100 K) [78], the unidentate ligands via S-donor atom with Br about each Cu(I) form a bent geometry of the S-Cu(I)-Br type. The

mean values of the Cu-L bond distances are 2.134 (±18) Å (L=S) and 2.234 (±8) Å (L=Br). The monoclinic [Cu($C_{21}H_{24}N_2S$)(I)] (at 298 K) [76] is the only example of the S-Cu(I)-I type. The Cu-L bond distances are 2.142 Å (L=S) and 2.385 Å (L=I). The S-Cu(I)-I bond angle is 160.7°.

There are two monoclinic Cu(I) complexes [Cu($C_{21}H_{24}N_2Se$)(Br)] (at 298 K) [76] and [Cu($C_{69}H_{56}N_2Se$)(Br)](C_7H_8) (at 100 K) [78] with an inner coordination sphere of the Se-Cu(I)Br type. The mean value of the Se-Cu(I)-Br angle is 164.2 (±9)°. The mean values of the Cu-L bond distances are 2.248 (±3) Å (L=Se) and 2.230 (±4) Å (L=Br).

The monoclinic [Cu($C_{21}H_{24}N_2Se$)(I)] (at 298 K) [76] is the only example with an inner coordination sphere of Se-Cu(I)-I. The structure is shown in Figure 8. The bent geometry respects the value of 159.6°. The Cu-L bond distances are 2.252 Å (L=Se) and 2.309 Å (L=I).

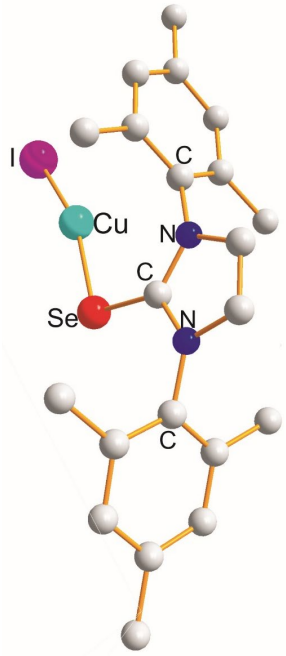

Figure 8. Structure of [Cu($C_{21}H_{24}N_2Se$)(I)] [76].

The monoclinic [Cu($C_{40}H_{47}N_2P$)(Cl)]0.5(C_7H_8) (at 173K) has an inner coordination sphere of the P-Cu(I)-Cl type [79]. The structure of the complex is shown in Figure 9.

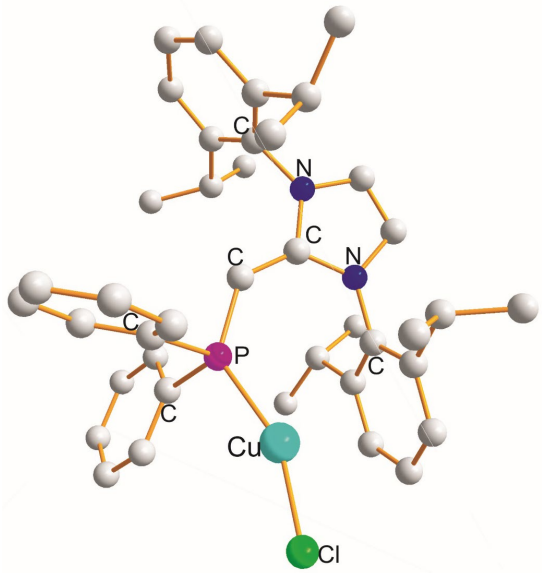

Figure 9. Structure of [Cu($C_{40}H_{47}N_2P$)(Cl)] 0.5 (C_7H_8) [79].

The value of the P-Cu(I)-Cl angle is 156.8°, and this indicates a bent geometry. The Cu-L bond distances are 2.120 Å (L=Cl) and 2.172 Å (L=P). The structure of the triclinic $[Cu(C_{40}H_{42}N_2P)(I)](C_7H_8)$ (at 173 K) [79] is similar to the chloride complex. The P-Cu-I angle is 144.5°and the Cu-L bond distances are 2.319 Å (L=I) and 2.202 Å (L=P).

The structures of $[Cu(C_{30}H_{42}N_4)(CH_3COO)]$ (at 213 K) [74] and $[Cu(C_{69}H_{56}N_2S)(Br)]C_7H_8$ (at 100 K) [78] are shown in Figures 10 and 11, respectively, as other illustrative examples of X-Cu(I)-Y complexes possessing X, Y with variable combinations of donor atoms.

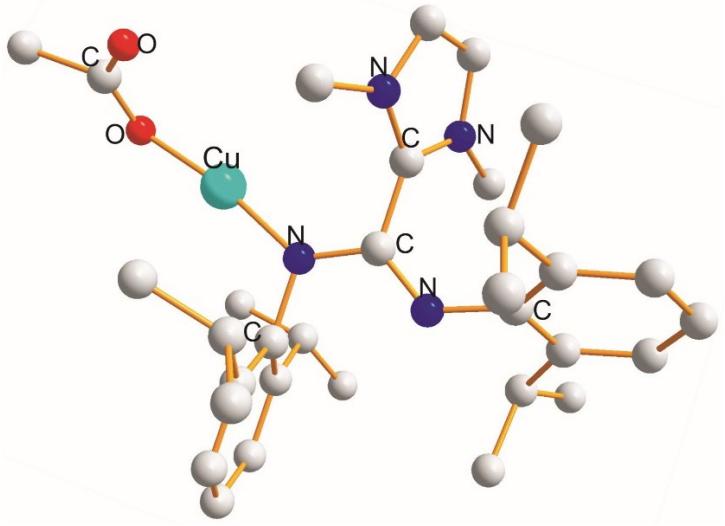

Figure 10. Structure of $[Cu(C_{30}H_{42}N_4)(CH_3COO)]$ [74].

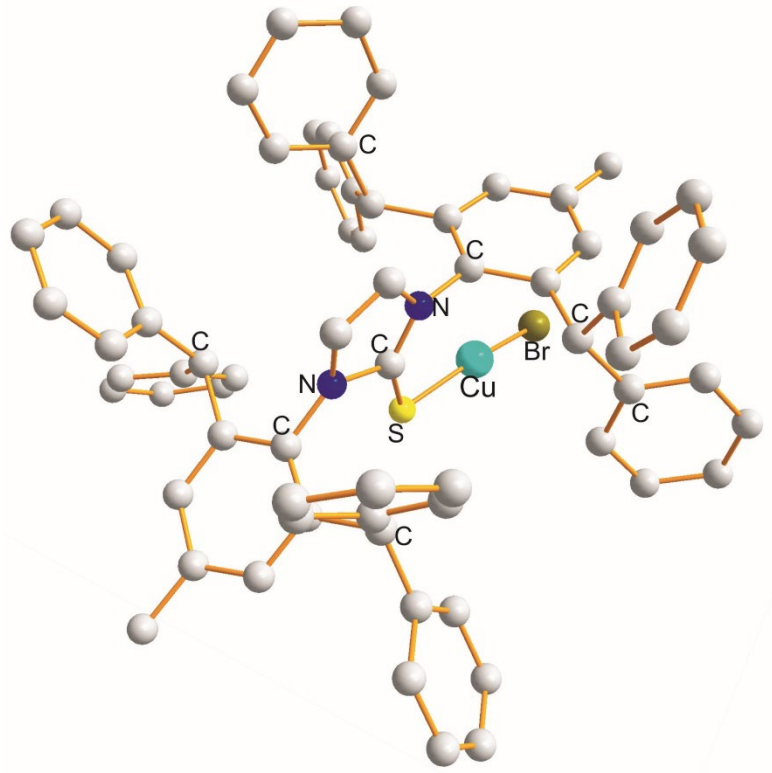

Figure 11. Structure of $[Cu(C_{69}H_{56}N_2S)(Br)]C_7H_8$ [78].

4. Conclusions

This structural study, employing Cambridge Crystallographic Database (CCDB) [80] for the analyzed structures and program Diamond [81] for creating chemical structure

vizualizations, classified over one hundredtwo-coordinate copper(I) complexes. It is known that there are two geometric possibilities for coordination number two, linear and bent, respectively. The former prevails in the structure of copper(I) compounds. In general, there are two preparative procedures: (i) direct reaction of the ligand and the copper(I) atom, and (ii) electrochemistry. Most syntheses have involved direct reaction between a copper(I) halide and the appropriate ligand in a non-aqueous solvent (such as acetonitrile) under an inert atmosphere. Over 80% of the X-rays measured were made at 100 K. It is noted that copper(I) complex cations can be isolated in salts with larger anions, both organic and inorganic: ClO_4, PF_4, SbF_6, BF_4, CF_3SO_3, and others.

The complexes crystallized in three crystal classes: monoclinic dominates with seventy-two examples, followed by triclinic (twenty-eight examples), and orthorhombic (eight examples). In the chemistry of "soft" copper(I), a wide variety of unidentate ligating atoms form two-coordinate Cu(I) complexes.

Over all, the mean Cu(I)-L distance is observed to increase with an increasing covalent radius of the ligating atom in the sequence 1.769 Å (H, 0.31 Å) < 1.838 Å (O, 0.6 Å) < 1.863 Å (N, 0.71 Å) < 1.904 Å (C, 0.76 Å) < 2.005 Å (B, 0.86 Å) < 2.101 Å (Cl, 1.00 Å) < 2.217 Å (S, 1.02 Å) < 2.219 Å (P, 1.06 Å) < 2.254 Å (Br, 1.14 Å) < 2.273 Å (Si, 1.17 Å) < 2.374 Å (Al, 1.21 Å) < 2.386 Å (I, 1.33 Å) < 2.474 Å (Sn, 1.40 Å).

A summary of the mean Cu(I)-L bond distances from the view of trans-effect is given in Table 1 and a summary of the mean X-Cu(I)-Y angles is given in Table 2.

Table 1. A summary of the mean Cu(I)-L bond distances [Å].

(X) [a] Trans to (Y) [b] [Å]	(X) Trans to (X) < [Å]	(X) [a] Trans to (Y) [b] [Å]
1.832 (C) < 1.848 (N)<	(O), 1.849, (O)	
1.852 (O) < 1.855 (Cl) < 1.864 (C)<	(N), 1.886, (N)	
2.095 (N) < 2.100 (C)<	(Cl), 2.104, (Cl)<	2.108 (S) < 2.120 (P)
2.104 (C) < 2.134 (Br)<	(S), 2.137, (S)<	2.139 (Cl) < 2.142 (I)
2.172 (Cl) < 2.202 (I) < 2.219 (C)<	(P), 2.236, (P)	
2.248 (Br) < 2.252 (I)<	(Se), 2.260, (Se)	
1.867 (S) < 1.869 (O) < 1.875 (N)<	(C), 1.900, (C)<	1.915 (I) < 1.917 (P) < 1.925 (Sn)<
1.879 (H) < 1.883 (Cl) < 1.892 (Br)		<1.935 (Si) < 1.939 (B) < 1.958 (Al)

[a] ligand affected defined in the central column [4]. [b] trans-effect ligand shown in parentheses.

Table 2. A summary of the mean X-Cu(I)-Y angles.

Organometalic Compounds C-Cu(I)-Y	Coordination Compounds X-Cu(I)-Y
178.9°(Y=I) > 177.8°(S) > 177.0°(H) > 175.9°(Al) > 175.8°(Cl) > 175.7°(N) > 175.1°(O) > 174.8°(Br) > 174.1°(P) > 173.7°(Si) > 173.5°(B) > 163.4°(Sn)	170.6°(X=N; Y=Cl) > 166.2°(S, Br) > 165.8°(S, Cl) > 164.2°(Se, Br) > 162.2°(N, O) > 160.7°(S, I) > 159.6°(Se, I) > 156.8°(P, Cl) > 144.5°(P, I)

The trans-effect on Cu(I) distances (trans to Y) can be divided into two categories. The first, left side of Table 1, is where a hetero-donor atom Y shortens the trans-Cu (I)-X bond, and the second, right side of Table 1, in which the Y-donor atom increases the length or weakness of the trans bond. These results suggest that in the former case, there is lower transfer of donor electrons from Y to Cu(I) than in the latter case. The "soft" atoms or ligands show a larger trans-effect than the borderline or "hard" ones. There are twenty-one varieties of inner coordination spheres about the copper(I) atoms.

These varieties can be divided into C-Cu(I)-Y and X-Cu(I)-Y. When the value of the C-Cu(I)-Y angle decreases, the deviation from the linearity increases in the sequence (mean values) given in Table 2. For X-Cu(I)-Y types, the sequence (mean values) is also given in Table 2.

For the comparison, in the series of mutually trans-X-Cu (I)-X complexes [15], the sequence is (mean values): 180.0°(X=Se) > 178.2°(S) > 175.5°(O) >175.9°(Cl) > 174.5°(N) > 174.0°(C) > 172.3°(P) > 169.7°(Br).

The maximum deviations from the linearity (180.0°) are (mean values) 10.3°(Br-Cu(I)-Br) > 16.6°(C-Cu(I)-Sn) < 35.50 (P-Cu(I)-I). As can be seen, the property of the ligand's increasing influence on deviation from linearity is in the order hard < borderline < soft.

Author Contributions: Conceptualization, M.M. and P.M.; methodology M.M. and P.M.; Writing—Original draft preparation, M.M. and P.M.; data curation, M.M.; Writing—Review and editing, V.M.; supervision, M.M. and P.M.; funding acquisition, P.M. All authors have read and agreed to the published version of the manuscript.

Funding: This work was supported by the project VEGA 1/0514/22, VEGA 1/0146/23 and KEGA 041UK-4/2024.

Data Availability Statement: The original contributions presented in the study are included in the article, further inquiries can be directed to the corresponding authors.

Acknowledgments: This work was supported by the Faculty of Pharmacy, Comenius University Bratislava. Structural data used in this study for discussion and calculations were obtained from Cambridge Crystallographic Database (CCDB) with an institutional license of the Slovak University of Technology in Bratislava.

Conflicts of Interest: The authors declare no conflicts of interest.

Abbreviations

2-CH_3py	2-methyl pyridine
2-Phpy	2-phenyl pyridine
$C_2H_3O_2$	acetate
C_4H_8O	tetrahydrofuran
$C_5H_{10}O_2B$	(5,5-dimethyl-1,3,2-dioxyborinan-2-yl)
$C_5H_3SO_2$	(thiophene-2-carboxylate)
$C_6H_{18}Si_2P$	bis(trimethylsilyl)phosphine
$C_6H_{23}N_2BP$	bis(diethylamino)phosphanido-borane)
C_7H_8	toluene
$C_8H_{10}N_2B$	(1,3-dimethyl-1,3,2-benzodiazaborol-2-yl)
$C_8H_{11}Si$	dimethyl(phenyl)silyl
$C_8H_4N_2$	(1,4-diisocyanobenzene)
$C_8H_5N_2O$	(benzoyliminomethylene amino)
$C_8H_7N_4O$	((4-methylphenyl)sulfonyl)carbamic azido)
$C_8H_7O_3$	4-methoxybenzoate
$C_9H_{16}N_2$	(1,3-bis(propan-2-yl)-imidazol-2-ylidene)
$C_{11}H_{10}F_4NO_2$	(t-butyl(2,3,5,6-tetrafluorophenyl)carbamatato)
$C_{11}H_{20}N_2$	(1,3-di-t-butyl-imidazol-2-ylidene)
$C_{11}H_{21}N_2$	(4,5-dimethyl-1,3-bis(propan-2-yl)-2,3-dihydro-1H-imidazol-2-ylidene)
$C_{11}H_{21}N_2$	(u-N,N-dipropan-2-ylmethylimidamide)-(4.5-dimethyl-1,3-bis(propan-2-yl)-2,3-dihydro-1H-imidazol-3-ylidene)
$C_{12}D_8N$	(perdeutero-9H-carbazol-9-yl)(1,3-bis(2,4,6-trimethylpephonyl)imidazol-2-ylidene)
$C_{12}H_8N$	(9H-carbazol-9-yl)
$C_{13}H_{19}N_3O_2$	(methyl-2-((bis((dimethylamino)methylidene)amino)benzoate)
$C_{14}H_{13}O_2$	(4-(4-methoxyphenyl)butanoate
$C_{16}H_{17}PON$	(1,1-diphenyl-N-(propan-2-yl)phosphanecarboxamidate)
$C_{18}H_{20}N_2$	(1,3-bis(2-methylphenyl)tetrahydropyrimiden-2-(1H)-ylidene
$C_{18}HBF_{15}$	hydrido(tris(pentafluorophenyl)borate
$C_{19}H_{20}N_2$	(1,3-bis(2,6-dimethylphenyl)imidazol-2-ylidene)
$C_{20}H_{24}N_2S$	(5-(4-(methylsulfanyl)phenyl)-1,3-di-isopropylbezimidazol-2-ylidene)
$C_{20}H_{31}N$	(1-(2,6-di-isopropylphenyl)-3,3′,5,5′-tetramethyl-pyrrolidin-2-ylidene)
$C_{20}H_{31}N$	4,5-dimethyl-1,3-bis(propan-2-yl)-2,3-dihydro-1H-imidazol-2-ylidene)
$C_{21}H_{16}N_2$	(1,3-bis(3-phenylprop-2-yn-1-yl)2,3-dihydro-1H-imidazol-2-ylidene)
$C_{21}H_{24}N_2$	(1,3-bis(mesityl)imidazol-2-ylidene)

$C_{21}H_{24}N_2S$	(1,3-bis(2,4,6-trimethylphenyl)1,3-dihydro-2H-imidazol-2-thione)
$C_{21}H_{24}N_2Se$	(1,3-bis(2,6-(2,4,6-trimethylphenyl)1,3-dihydro-2H-imidazole-2-selone)
$C_{21}H_{24}P$	(tris(4-methylyphenylphosphine)
$C_{21}H_{26}N_2$	(1,3-dimesitylimidazolidin-2-ylidene)
$C_{21}H_{32}N_4$	(1-(2-(dimethylamino)ethyl)-3-(N-(2,6-bis(propan-2-yl)phenyl)ethaniminodoyl)-2,3dihydro-1H-imidazil-2-ylidene)
$C_{22}H_{21}F_5N_2$	(1-(2,6-di-isopropylphenyl)-3-((pentafluorophenylmethyl)imidazol-2-ylidene)
$C_{22}H_{33}N$	(2-(2,6-di-isopropylphenyl)-1,4,5-trimethyl-2-azabiyclo [2.2.2]octan-3-ylidene
$C_{22}H_{35}N$	(1-(2,6-di-isopropylphenyl)-3,3-diethyl-5,5-dimethylpyrolidin-2-ylidene)
$C_{22}H_{36}N$	((1-(2,6-di-isopropyl)-4,4-diethyl-2,2-dimethyl-3,4-dihydro-2H-pyrrol-1-ium
$C_{22}H_{39}N_4OP$	(1,3-dicyclohexyl-4,6-bis(cycohexylimino)-2-oxo-1,3,5-diazaphophinan-5-yl)
$C_{23}H_{35}N$	(9H-carbazol-9-yl)-2-(2,6-di-isopropylphenyl)-3,3-dimethyl-2-araspirio
$C_{24}H_{26}N_2O_2$	(1,3-dimesilyl-5,5-dimethyl-4,6-doxohexahydropyrimidin-2-yl)
$C_{24}H_{28}N_2O_2$	(1,3-dimesityl-5,5-dimethyl-4,6-dioxotetrahydropyrimidin-2(1H)-ylidene)
$C_{27}H_{30}N_2$	(1-(2,6-bis(propan-2-yl)phenyl)-3-(1-naphalen-1-yl)ethyl)2,3-dihydro-1H-imidazol-2-yl)
$C_{27}H_{36}N_2$	(1,3-bis(2,6-di-isopropylphenyl)imidazol-2-ylidene)
$C_{27}H_{36}N_2O_2$	(2,3-bis(2,6-diisopropylphenyl)amino)acrylate)
$C_{27}H_{36}N_2S$	(1,3-bis(2,6-diisopropylphenyl)-1,3-dihydro-2H-imidazol-2-thione)
$C_{27}H_{37}N_2$	(1,3-bis(2,6-disopropylphenyl)imidazol-2-ylidene)
$C_{27}H_{38}N_2$	(1,3-bis(2,6-di-isopropylphenyl)-4,5-dihydroimidazol-2-ylidene)
$C_{27}H_{39}N$	(1-(2,6-di-isopropylphenyl)-5,5-dimethyl-2H-spirolpyrolidine-3,2-tricyclo [3.3.1.1.^{3,7}]decan(2-ylidene)
$C_{27}H_{40}N$	(1-(2,6-diisopropylphenyl)-3,3-diethyl-5,5-dimethylpyrolidin-2-ylidene
$C_{27}H_{43}N$	(2-(2,6-bis(propan-2-yl)phenyl)-3,3,9-trimethyl-6-propan-2-yl)-2-azaspiro(4,5) decan-1-ylidene
$C_{27}H_{46}N_2O_3Si$	(1-(2,6-diisopropylphenyl)-3-(3-(trisopropoxysilyl)propyl)imidazol-2-ylidene)
$C_{28}H_{39}N_2$	(1,3-bis[2,6-bis(propan-2-yl)phenyl)-1,3-diazinan-2-ylidene)
$C_{28}H_{40}N_2$	(1,3-bis[2,6-bis(propan-2-yl)phenyl]tetrahydro-pyrimidin-2(1H)-ylidene)
$C_{30}H_{42}N_4$	(2-(N,N-bis(2,6-diisopropylphenyl))carbammidoyl)-1,3-dimethyl-1H-imidazol-3-iumato)
$C_{30}H_{42}N_6$	(4-((2-azidoethyl)(methyl)amino)-1,3-bis(2,6-di-isopropylphenyl)-2,3-dihydro-1H-imidazol-2-ilydene)
$C_{30}H_{49}N_2Si_2Al$	((ethane-1,2-diyl)bis(N-[2,6-bis(propan-2-yl)phenyl))-1,1-dimethylsilanamino)) aluminium
$C_{30}H_{50}N_2Si_2Al$	((ethane-1,2-diyl)bis(N-[2,6-bis(popan-2-yl)phenyl)1,1-dimethylsilanamino)) aluminium)
$C_{30}H_{56}B_{11}N_3$	(2-(3-t-butyl-2-(2,6-di-isopropylphenyl)-1-(1,3-di-isopropyl-4,5-dimethylimidazol-2-ylidene)-2,1-azaborinyl)1,2-dicarbo-closo-dodecaboran-2-yl)
$C_{31}H_{32}N_2$	(2,4-dimesityl-1,2,4,5-tetrahydro-3H-naphtho[1,8-ef] [1,3]diazoein-3-ylidene)
$C_{31}H_{38}N_2$	(1,3-bis(2,6-bis(propan-2-yl)phenyl-2,3-dihydro-1H-benzimidazol-2-ylidene)
$C_{32}H_{31}N$	(2-(2,6-bis(propan-2-yl)phenyl)-3,3-diphenyl-2,3-dihydro-1H-isoindol-1-ylidene)
$C_{35}H_{36}N_2$	(2,3-bis(bis(1-phenylethyl)amino)cycloprop-2-en-1-ylidene)
$C_{37}H_{63}AlN_4Si_2$	(ethane-1,2-diyl)bis(N-[2,6-bis(propan-2-yl)phenyl]-1,1-dimethyl-silanamino)-aluminium)
$C_{40}H_{47}N_2Cl$	(4-chloro-1,3-bis(2,6-di-isopropylphenyl)-5-methyl(diphenylphosphono)-imidazol-2-ylidene)
$C_{40}H_{47}N_2P$	(2-((diphenylphosphanyl)-1,3-bis(2,6-bis(propan-2-yl)phenyl)2,3-dihydro-1H-imidazole)
$C_{40}H_{58}N_4$	(2-N,N-bis(2,6-diisopropylphenyl)(carbamimidoyl)-1,3-dicyclohexyl)-1H-imidazol-3-iumato)
$C_{41}H_{38}N_2O_2$	(R,R)-(1,3-bis(8-(4-methocyphenyl)-1,2,3,4-tetrahydronaphthalen-1-yl) benzimidazol-2-ylidene)
$C_{45}H_{40}N_2$	(1,3-bis(2-(diphenylmethyl)-4,6-dimethyl-phenyl)-imidazol-2-ylidene)
$C_{45}H_{42}N_2$	(1,3-bis(2-(diphenylmethyl-4,6-dimethylphenyl)imidazolidin-2-ylidene)
$C_{55}H_{44}N_2$	(7,9-bis(4-(diphenylmethyl)-2,6-dimethylphenyl)-8,9-dihydro-7H-acenaphlo [1,2-d]imidazol-8-ylidene)

$C_{60}H_{84}AlN_4O$	(u-N-(cyclohexyl)((cyclohexyl)amino)methanidamido)-(2,7-di-t-butyl-N^4,N^5-bis(2,6-bis(propan-2-yl)phenyl)-9,9-dimethyl-9H-xanthene-4,5-bis(amido) aluminium)
$C_{69}H_{56}N_2$	(1,3-bis(2,6-bis(diphenylmethyl)-4-methylphenyl)imidazol-2-ylidene)
$C_{69}H_{56}N_2S$	(1,3-bis(2,6-bis(diphenylmethyl)-4-methylphenyl)-1,3-dihydro-2H-imidazol-2-thione
$C_{69}H_{56}N_2Se$	(1,3-bis(2,6-bis(diphenylmethyl)-4-methylphenyl)-1,3-dihydro-2H-imidazole-2-selone
CHO_2	formate
Ph_2P	diphenylphophido
Ph_3Si	triphenylsilyl
Ph_3SiO	triphenylsilanolate
PhCOO	benzoate
py	pyridine
t-Bu_3 P=N	(tri-t-butylphosphanylidene)azanide
t-Bu_3P	tri-t-bitylphosphine

References

1. Österberg, R. Models for copper-protein interaction based on solution and crystal structure studies. *Coord. Chem. Rev.* **1974**, *12*, 309–347. [CrossRef]
2. Colman, P.M.; Freeman, H.C.; Guss, J.M.; Murata, M.; Norris, B.A.; Ramshaw, J.A.M.; Venkatappa, M.P. X-ray crystal structure analysis of plastocyanin at 2.7 Å resolution. *Nature* **1978**, *272*, 319–324. [CrossRef]
3. Spiro, T.G. *Copper Proteins*, 1st ed.; Krieger Pub. Co. Publisher: Malabar, FL, USA, 1981; p. 376.
4. Dockal, E.R.; Diaddario, L.L.; Glick, M.D.; Rorabacher, D.B. Structure of 1,4,8,11-tetrathiacyclotetradecanecopper(I) perchlorate: Comparative geometries of analogous copper(I) and copper(II) complexes. *J. Am. Chem. Soc.* **1977**, *99*, 4530–4532. [CrossRef]
5. Baker, E.N.; Norris, G.E. Copper co-ordination to thioether ligands: Crystal and molecular structures of bis(2,5-dithiahexane)copper(II) bis(tetrafluoroborate) and bis(3,6-dithiaoctane)copper(I) tetrafluoroborates. *J. Chem. Soc. Dalton Trans.* **1977**, *24*, 877–882. [CrossRef]
6. Olmstead, M.M.; Musker, W.K.; Kessler, R.M. Crystal structures and properties of bis(2,5-dithiahexane)copper(I) and copper(II) and mixed-valence complexes. Comparison of tetrahedral and distorted octahedral geometries of thioether-coordinated copper(II). *Inorg. Chem.* **1981**, *20*, 151–157. [CrossRef]
7. Henriksson, H.A.; Sjöberg, B.; Österberg, R. Model structures for a copper(I)–copper(II) redox couple in copper proteins: *X*-ray powder structure of bis(imidazole)copper(I) perchlorate and crystal structure of bis(imidazole)copper(II) diacetate. *J. Chem. Soc. Chem. Commun.* **1976**, *4*, 130–131. [CrossRef]
8. Ainscough, E.W.; Baker, E.N.; Brodie, A.M.; Larsen, N.G. Copper co-ordination to thioether ligands. Spectroscopic studies of dimeric copper(II) complexes of 2-(3,3-dimethyl-2-thiabutyl)pyridine and the crystal structure of di-μ-bromo-bis{bromo[2-(3,3-dimethyl-2-thiabutyl)pyridine-NS]copper(II)}. *J. Chem. Soc. Dalton Trans.* **1981**, *10*, 2054–2058. [CrossRef]
9. Hathaway, B.J. Copper. *Coord. Chem. Rev.* **1981**, *35*, 211–252. [CrossRef]
10. Hathaway, B.J. Copper. *Coord. Chem. Rev.* **1982**, *41*, 423–487. [CrossRef]
11. Hathaway, B.J. Copper. *Coord. Chem. Rev.* **1983**, *52*, 87–169. [CrossRef]
12. O'Brien, P. Copper. *Coord. Chem. Rev.* **1984**, *58*, 169–244. [CrossRef]
13. Caulton, K.G.; Davies, G.; Holt, E.M. Synthesis, molecular structures, properties and reactions of halo- and carbonyl(amine)copper(I) complexes. *Polyhedron* **1990**, *9*, 2319–2351. [CrossRef]
14. Holloway, C.E.; Melník, M. Copper(I) compounds: Classification and analysis of crystallographic and structural data. *Rev. Inorg. Chem.* **1995**, *15*, 147–386. [CrossRef]
15. Melník, M.; Mikušová, V.; Mikuš, P. The structural aspects of mutually trans-X–Cu(I)–X (X=OL, NL, CL, PL, SL, SeL, Cl or Br) complexes. *Inorganics* **2024**, *12*, 245. [CrossRef]
16. Romero, E.A.; Zhao, T.; Nakano, R.; Hu, X.; Wu, Y.; Jazzar, R.; Bertrand, G. Tandem copper hydride–Lewis pair catalysed reduction of carbon dioxide into formate with dihydrogen. *Nat. Catal.* **2018**, *1*, 743–747. [CrossRef]
17. Hall, J.W.; Unson, D.M.L.; Brunel, P.; Collins, L.R.; Cybulski, M.K.; Mahon, M.F.; Whittlesey, M.K. Copper-NHC-Mediated Semi-Hydrogenation and Hydroboration of Alkynes: Enhanced Catalytic Activity Using Ring-Expanded Carbenes. *Organometallics* **2018**, *37*, 3102–3110. [CrossRef]
18. Jones, C.; Mills, D.P.; Rose, R.P.; Stasch, A.; Woodul, W.D. Synthesis and further reactivity studies of some transition metal gallyl complexes. *J. Organomet. Chem.* **2010**, *695*, 2410–2417. [CrossRef]
19. Mankad, N.P.; Gray, T.G.; Laitar, D.S.; Sadighi, J.P. Synthesis, Structure, and CO_2 Reactivity of a Two-Coordinate (Carbene)copper(I) Methyl Complex. *Organometallics* **2004**, *23*, 1191–1193. [CrossRef]
20. Goj, L.A.; Blue, E.D.; Delp, S.A.; Gunnoe, T.B.; Cundari, T.R.; Petersen, J.L. Single-Electron Oxidation of Monomeric Copper(I) Alkyl Complexes: Evidence for Reductive Elimination through Bimolecular Formation of Alkanes. *Organometallics* **2006**, *25*, 4097–4104. [CrossRef]

21. Nolte, C.; Mayer, P.; Straub, B.F. Isolation of a copper(I) triazolide: A "click" intermediate. *Angew. Chem. Int. Ed.* **2007**, *46*, 2101–2103. [CrossRef]
22. McReynolds, K.A.; Lewis, R.S.; Ackerman, L.K.G.; Dubinina, G.G.; Brennessel, W.W.; Vicic, D.A. Decarboxylative Trifluoromethylation of Aryl Halides Using Well-Defined Copper-Trifluoroacetate and –Chlorodifluoroacetate Precursors. *J. Fluorine Chem.* **2010**, *131*, 1108–1112. [CrossRef]
23. Bhattacharyya, K.X.; Akana, J.A.; Laitar, D.S.; Berlin, J.M.; Sadighi, J.P. Carbon−Carbon Bond Formation on Reaction of a Copper(I) Stannyl Complex with Carbon Dioxide. *Organometallics* **2008**, *27*, 2682–2684. [CrossRef]
24. Ohishi, T.; Nishiura, M.; Hou, Z. Carboxylation of Organoboronic Esters Catalyzed by N-Heterocyclic Carbene Copper(I) Complexes. *Angew. Chem. Int. Ed.* **2008**, *47*, 5792–5795. [CrossRef] [PubMed]
25. Shi, S.; Collins, L.R.; Mahon, M.F.; Djurovich, P.I.; Thompson, M.E.; Whittlesey, M.K. Synthesis and characterization of phosphorescent two-coordinate copper(i) complexes bearing diamidocarbene ligands. *Dalton Trans.* **2017**, *46*, 745–752. [CrossRef]
26. Yang, W.J.; Kang, B.N.; Lee, J.H.; Choi, Y.M.; Kim, C.H.; Yun, J. NHC-copper-thiophene-2-carboxylate complex for the hydroboration of terminal alkynes. *Org. Biomol. Chem.* **2019**, *17*, 5249–5252. [CrossRef]
27. Ohishi, T.; Zhang, L.; Nishiura, M.; Hou, Z. Carboxylation of alkylboranes by N-heterocyclic carbene copper catalysts: Synthesis of carboxylic acids from terminal alkenes and carbon dioxide. *Angew. Chem. Int. Ed.* **2011**, *50*, 8114–8117. [CrossRef]
28. Liske, A.; Wallbaum, L.; Holzel, T.; Foller, J.; Gernert, M.; Hupp, B.; Ganter, C.; Marian, C.M.; Steffen, A. Cu-F Interactions between Cationic Linear N-Heterocyclic Carbene Copper(I) Pyridine Complexes and Their Counterions Greatly Enhance Blue Luminescence Efficiency. *Inorg. Chem.* **2019**, *58*, 5433–5445. [CrossRef]
29. Bai, T.; Yang, Y.; Han, C. Isolation and characterization of hydrocarbon soluble NHC copper(I) phosphoranimide complex and catalytic application for alkyne hydroboration reaction. *Tetrahedron Lett.* **2017**, *58*, 1523–1527. [CrossRef]
30. Tzouras, N.V.; Martynova, E.A.; Ma, X.; Scattolin, T.; Hupp, B.; Busen, H.; Saab, M.; Zhang, Z.; Falivene, L.; Pisano, G.; et al. Simple Synthetic Routes to Carbene-M-Amido (M=Cu, Ag, Au) Complexes for Luminescence and Photocatalysis Applications. *Chem. A Eur. J.* **2021**, *27*, 11904–11911. [CrossRef]
31. Downie, T.M.H.; Hall, J.W.; Finn, T.P.C.; Liptrot, D.J.; Lowe, J.P.; Mahon, M.F.; McMullin, C.J.; Whittlesey, M.K. The first ring-expanded NHC–copper(i) phosphides as catalysts in the highly selective hydrophosphination of isocyanates. *Chem. Commun.* **2020**, *56*, 13359–13362. [CrossRef]
32. Hamze, R.; Idris, M.; Ravinson, D.S.M.; Jung, M.C.; Haiges, R.; Djurovich, P.I.; Thompson, M.E. Highly Efficient Deep Blue Luminescence of 2-Coordinate Coinage Metal Complexes Bearing Bulky NHC Benzimidazolyl Carbene. *Front. Chem.* **2020**, *8*, 535809. [CrossRef] [PubMed]
33. Trose, M.; Nahra, F.; Cordes, D.B.; Slawin, A.M.Z.; Cazin, C.S.J. Cu–NHC azide complex: Synthesis and reactivity. *Chem. Commun.* **2019**, *55*, 12068–12071. [CrossRef] [PubMed]
34. Li, J.; Wang, L.; Zhao, Z.; Li, X.; Yu, X.; Huo, P.; Jin, Q.; Liu, Z.; Brian, Z.; Huang, C. Two-Coordinate Copper(I)/NHC Complexes: Dual Emission Properties and Ultralong Room-Temperature Phosphorescence. *Angew. Chem. Int. Ed.* **2020**, *59*, 8210–8217. [CrossRef] [PubMed]
35. Dodds, C.A.; Kennedy, A.R.; Thompson, R. Taming Copper(I) Cyanate and Selenocyanate with N-Heterocyclic Carbenes. *Eur. J. Inorg. Chem.* **2019**, *2019*, 3581–3587. [CrossRef]
36. Xie, W.; Yoon, J.H.; Chang, S. (NHC)Cu-Catalyzed Mild C–H Amidation of (Hetero)arenes with Deprotectable Carbamates: Scope and Mechanistic Studies. *J. Am. Chem. Soc.* **2016**, *138*, 12605–12614. [CrossRef]
37. Liu, H.Y.; Schwamm, R.J.; Hill, M.S.; Mahon, M.F.; McMullin, C.L.; Rajabi, N.A. Ambiphilic Al-Cu Bonding. *Angew. Chem. Int. Ed.* **2021**, *60*, 14390–14393. [CrossRef]
38. Zhai, Y.; Filatov, A.S.; Hillhouse, G.L.; Hopkins, M.D. Synthesis, structure, and reactions of a copper–sulfido cluster comprised of the parent Cu_2S unit: $\{(NHC)Cu\}_2(\mu\text{-}S)$. *Chem. Sci.* **2016**, *7*, 589–595. [CrossRef]
39. McCarly, B.Y.; Thomas, B.M.; Zeller, M.; Van Hoveln, R. Synthesis of a Copper Silyl Complex by Disilane Activation. *Organometallics* **2018**, *37*, 2937–2940. [CrossRef]
40. Plotzitzka, J.; Kleeberg, C. $[(NHC)Cu^{I}\text{–}ER_3]$ Complexes (ER_3 = $SiMe_2Ph$, $SiPh_3$, $SnMe_3$): From Linear, Mononuclear Complexes to Polynuclear Complexes with Ultrashort $Cu^{I}\cdots Cu^{I}$ Distances. *Inorg. Chem.* **2016**, *55*, 4813–4823. [CrossRef]
41. Parvin, N.; Hossain, Y.; George, A.; Parameswaran, P.; Khan, S. N-heterocyclic silylene stabilized monocordinated copper(i)–arene cationic complexes and their application in click chemistry. *Chem. Commun.* **2020**, *56*, 273–276. [CrossRef]
42. Kleeberg, C.; Borner, C. Syntheses, Structures, and Reactivity of NHC Copper(I) Boryl Complexes: A Systematic Study. *Organometallics* **2018**, *37*, 4136–4146. [CrossRef]
43. Drescher, W.; Borner, C.; Kleeberg, C. Stability and decomposition of copper(I) boryl complexes: [(IDipp)Cu–Bneop], [(IDipp*)Cu–Bneop] and copper clusters. *New. J. Chem.* **2021**, *45*, 14957–14964. [CrossRef]
44. Najafabadi, B.K.; Corrigan, J.F. Enhanced thermal stability of Cu–silylphosphido complexes *via* NHC ligation. *Dalton Trans.* **2015**, *44*, 14235–14241. [CrossRef] [PubMed]
45. Liu, L.L.; Ruiz, D.A.; Dahcheh, F.; Bertrand, G.; Suter, R.; Tondreau, A.M.; Grutzmacher, H. Isolation of Au-, Co-η^1PCO and Cu-η^2PCO complexes, conversion of an Ir–η^1PCO complex into a dimetalladiphosphene, and an interaction-free PCO anion. *Chem. Sci.* **2016**, *7*, 2335–2341. [CrossRef]
46. Blum, M.; Kappler, J.; Schlindwein, S.H.; Nieger, M.; Gudat, D. Synthesis, spectroscopic characterisation and transmetalation of lithium and potassium diaminophosphanide-boranes. *Dalton Trans.* **2018**, *47*, 112–119. [CrossRef]

47. McManus, C.; Hicks, J.; Cui, X.; Zhao, L.; Frenking, G.; Goicoechea, J.M.; Aldridge, S. Coinage metal aluminyl complexes: Probing regiochemistry and mechanism in the insertion and reduction of carbon dioxide. *Chem. Sci.* **2021**, *12*, 13458–13468. [CrossRef]
48. Collins, L.R.; Riddlestone, I.M.; Mahon, M.F.; Whittlesey, M.K. A comparison of the stability and reactivity of diamido- and diaminocarbene copper alkoxide and hydride complexes. *Chem. Eur. J.* **2015**, *21*, 14075–14084. [CrossRef]
49. Kuehn, L.; Eichhorn, A.F.; Marder, T.B.; Radius, U. Copper(I) complexes of *N*-alkyl-substituted N-Heterocyclic carbenes. *J. Organomet. Chem.* **2019**, *881*, 25–33. [CrossRef]
50. Rasale, D.; Patil, K.; Sauter, B.; Geigle, S.; Zhanybekova, S.; Gillingham, D. A new water soluble copper N-heterocyclic carbene complex delivers mild O^6G-selective RNA alkylation. *Chem. Commun.* **2018**, *54*, 9174–9177. [CrossRef]
51. Manar, K.K.; Chakrabortty, S.; Porwal, V.K.; Prakash, D.; Thakur, S.K.; Choudhury, A.R.; Singh, S. Two-Coordinate Cu (I) and Au (I) Complexes Supported by BICAAC and CAAC Ligands. *ChemistrySelect* **2020**, *5*, 9900–9907. [CrossRef]
52. Shaw, P.; Kennedy, A.R.; Nelson, D.J. Synthesis and characterisation of an N-heterocyclic carbene with spatially-defined steric impact. *Dalton Trans.* **2016**, *45*, 11772–11780. [CrossRef] [PubMed]
53. Laidlaw, G.; Wood, S.H.; Kennedy, A.R.; Nelson, D.J. An N-Heterocyclic Carbene with a Saturated Backbone and Spatially-Defined Steric Impact. *Z. Anorg. Allg. Chem.* **2019**, *645*, 105–112. [CrossRef]
54. Dodds, C.A.; (University of Glasgow, Glasgow, UK); Kennedy, A.R.; (University of Strathclyde, Glasgow, UK). Personal communication, 2018.
55. Doud, E.A.; Inkpen, M.S.; Lovat, G.; Montes, E.; Paley, D.W.; Steigerwald, M.L.; Vazquez, H.; Venkataraman, L.; Roy, X. In Situ Formation of N-Heterocyclic Carbene-Bound Single-Molecule Junctions. *J. Am. Chem. Soc.* **2018**, *140*, 8944–8949. [CrossRef] [PubMed]
56. Romanov, A.S.; Becker, C.R.; James, C.E.; Di, D.; Credgington, D.; Linnolahti, M.; Bochmann, M. Copper and Gold Cyclic (Alkyl)(amino)carbene Complexes with Sub-Microsecond Photoemissions: Structure and Substituent Effects on Redox and Luminescent Properties. *Chem. A Eur. J.* **2017**, *23*, 4625–4637. [CrossRef]
57. Ren, X.; Wesolek, M.; Braunstein, P. Cu(i), Ag(i), Ni(ii), Cr(iii) and Ir(i) complexes with tritopic $N^{imine}C^{NHC}N^{amine}$ pincer ligands and catalytic ethylene oligomerization. *Dalton Trans.* **2019**, *48*, 12895–12909. [CrossRef]
58. Wang, H.; Zhang, J.; Xie, Z. Reversible Photothermal Isomerization of Carborane-Fused Azaborole to Borirane: Synthesis and Reactivity of Carbene-Stabilized Carborane-Fused Borirane. *Angew. Chem. Int. Ed.* **2017**, *56*, 9198–9201. [CrossRef]
59. Deng, M.; Mukthar, N.F.M.; Schley, N.D.; Ung, G. Yellow Circularly Polarized Luminescence from C_1 -Symmetrical Copper(I) Complexes. *Angew. Chem. Int. Ed.* **2020**, *59*, 1228–1231. [CrossRef]
60. Romanov, A.S.; Di, D.; Yang, L.; Fernandez-Cestau, J.; Becker, C.R.; James, C.E.; Zhu, B.; Linolahti, M.; Credgington, D.; Bochmann, M. Highly photoluminescent copper carbene complexes based on prompt rather than delayed fluorescence. *Chem. Commun.* **2016**, *52*, 6379–6382. [CrossRef]
61. Liu, C.; Shen, H.Q.; Chen, M.W.; Zhou, Y.G. C_2-Symmetric Hindered "Sandwich" Chiral *N*-Heterocyclic Carbene Precursors and Their Transition Metal Complexes: Expedient Syntheses, Structural Authentication, and Catalytic Properties. *Organometallics* **2018**, *37*, 3756–3769. [CrossRef]
62. Tarrieu, R.; Dumas, A.; Thongpaen, J.; Vives, T.; Roisnel, T.; Dorcet, V.; Crevisy, C.; Basle, O.; Mauduit, M. Readily accessible unsymmetrical unsaturated 2, 6-diisopropylphenyl N-heterocyclic carbene ligands. Applications in enantioselective catalysis. *J. Org. Chem.* **2017**, *82*, 1880–1887. [CrossRef]
63. Pan, T.; Wang, Y.; Liu, F.S.; Lin, H.; Zhou, Y. Copper(I)–NHCs complexes: Synthesis, characterization and their inhibition against the biofilm formation of *Streptococcus mutans*. *Polyhedron* **2021**, *197*, 115033. [CrossRef]
64. Pape, F.; Brechmann, L.T.; Teichert, J.F. Catalytic Generation and Chemoselective Transfer of Nucleophilic Hydrides from Dihydrogen. *Chem. Eur. J.* **2019**, *25*, 985–988. [CrossRef] [PubMed]
65. Lorkowski, J.; Krahfuss, M.; Kubicki, M.; Radius, U.; Pietraszuk, C. Intramolecular Ring-Expansion Reaction (RER) and Intermolecular Coordination of In Situ Generated Cyclic (Amino)(aryl)carbenes (cAArCs). *Chem. Eur. J.* **2019**, *25*, 11365–11374. [CrossRef] [PubMed]
66. Kiefer, C.; Bestgen, S.; Gamer, M.T.; Kuhn, M.; Lebedkin, S.; Weigend, F.; Kappes, M.M.; Roesky, P.W. Coinage Metal Complexes of Bis-Alkynyl-Functionalized N-Heterocyclic Carbenes: Reactivity, Photophysical Properties, and Quantum Chemical Investigations. *Chem. Eur. J.* **2017**, *23*, 1591–1603. [CrossRef] [PubMed]
67. Schwedtmann, K.; Schoemaker, R.; Hennersdorf, F.; Bauza, A.; Fontera, A.; Weiss, R.; Weigand, J.J. Cationic 5-phosphonio-substituted N-heterocyclic carbenes. *Dalton Trans.* **2016**, *45*, 11384–11396. [CrossRef]
68. Delgado-Rebollo, M.; Garcia-Morales, C.; Maya, C.; Prieto, A.; Echavarren, A.M.; Perez, P.J. Coinage metal complexes bearing fluorinated N-Heterocyclic carbene ligands. *J. Organomet. Chem.* **2019**, *898*, 120856. [CrossRef]
69. Chesnokov, G.A.; Dzhevakov, P.B.; Rybakov, V.B.; Nechaev, M.S.; (M. V. Lomonosov Moscow State University, Moscow, Russia); Topchiy, M.A.; Gribanov, P.S.; Asachenko, A.F.; (Russian Academy of Sciences, Moscow, Russia); Khrustalev, V.N.; (Peoples' Friendship University of Russia, Moscow, Russia). Personal communication, 2016.
70. Gernert, M.; Balles-Wof, L.; Kerner, F.; Muller, U.; Schmiedel, A.; Holzapfel, M.; Marian, C.M.; Pflaum, J.; Lambert, C.; Steffen, A. Cyclic (Amino)(aryl)carbenes Enter the Field of Chromophore Ligands: Expanded π System Leads to Unusually Deep Red Emitting Cu^I Compounds. *J. Am. Chem. Soc.* **2020**, *142*, 8897–8909. [CrossRef]
71. Garces, K.; Fernandez-Alvarez, F.J.; Garcia-Orduna, P.; Lahoz, F.J.; Perez-Torrente, J.J.; Oro, L.A. Grafting of Copper(I)–NHC Species on MCM-41: Homogeneous versus Heterogeneous Catalysis. *ChemCatChem* **2015**, *7*, 2501–2507. [CrossRef]

72. Hayakawa, T.; Sakata, T.; (Josai University, Saitama, Japan). Personal communication, 2017.
73. Jones, P.G.; Holschumacher, D.; Hrib, C.G.; Tamm, M.; (Technische Universität Carolo-Wilhelmina, Braunschweig, Germany). Personal communication, 2019.
74. Marquez, A.; Avila, E.; Urbaneja, C.; Alvarez, E.; Palma, P.; Campora, J. Copper(I) Complexes of Zwitterionic Imidazolium-2-Amidinates, a Promising Class of Electroneutral, Amidinate-Type Ligands. *Inorg. Chem.* **2015**, *54*, 11007–11017. [CrossRef]
75. Florke, U.; (Universität Paderborn, Paderborn, Germany); Nagel, C.; (Julius-Maximilians-Universität Würzburg, Würzburg, Germany); Henkel, G.; (Westfälische Wilhelms-Universität Münster, Münster, Germany). Personal communication, 2017.
76. Srinivas, K.; Prabusankar, G. Role of C, S, Se and P donor ligands in copper(i) mediated C–N and C–Si bond formation reactions. *RSC Adv.* **2018**, *8*, 32269–32282. [CrossRef]
77. Rheingold, A.L.; (University of California, San Diego, CA, USA); Rabinovich, D.; (The University of North Carolina at Charlotte, Charlotte, NC, USA); Golen, J.A.; (University of Massachusetts Dartmouth, North Dartmouth, MA, USA). Personal communication, 2020.
78. Parvin, N.; Pal, S.; Khan, S.; Das, S.; Pati, S.K.; Roesky, H.W. Unique approach to copper(I) silylene chalcogenone complexes. *Inorg. Chem.* **2017**, *56*, 1706–1712. [CrossRef] [PubMed]
79. Lui, M.W.; Shynkaruk, O.; Oakley, M.S.; Sinelnikov, R.; McDonald, R.; Ferguson, M.J.; Meldrum, A.; Klobukowski, M.; Rivard, E. Engaging dual donor sites within an N-heterocyclic olefin phosphine ligand. *Dalton Trans.* **2017**, *46*, 5946–5954. [CrossRef] [PubMed]
80. Groom, C.R.; Allen, F.H. The Cambridge Structural Database in Retrospect and Prospect. *Angew. Chem. Int. Ed.* **2014**, *53*, 662–671. [CrossRef] [PubMed]
81. Brandenburg, K.; Putz, H.; Berndt, M. *DIAMOND*; Crystal Impact GbR: Bonn, Germany, 1999.